Bull. Mater. Sci., Vol. 22, No. 3, May 1999, pp. 321–327. © Indian Academy of Sciences.

Alloying behaviour in nanocrystalline materials during mechanical alloying

S K PABI*, I MANNA and B S MURTY

Department of Metallurgical and Materials Engineering, Indian Institute of Technology, Kharagpur 721 302, India

Abstract. **The alloying behaviour in a number of systems such as Cu–Ni, Cu–Zn, Cu–Al, Ni–Al, Nb–Al has been studied to understand the mechanism as well as the kinetics of alloying during mechanical alloying (MA). The results show that nanocrystallization is a prerequisite for alloying in all the systems during MA. The mechanism of alloying appears to be a strong function of the enthalpy of formation of the phase and the energy of ordering in case of intermetallic compounds. Solid solutions (Cu–Ni), intermetallic compounds with low ordering energies (such as Ni_3Al which forms in a disordered state during MA) and compounds with low enthalpy of formation (Cu–Zn, Al_3Nb) form by continuous diffusive mixing. Compounds with high enthalpy of formation and high ordering energies form by a new mechanism christened as discontinuous additive mixing. When the intermetallic gets disordered, its formation mechanism changes from discontinuous additive mixing to continuous diffusive one. A rigorous mathematical model, based on iso-concentration contour migration method, has been developed to predict the kinetics of diffusive intermixing in binary systems during MA. Based on the results of Cu–Ni, Cu–Zn and Cu–Al systems, an effective temperature (T_{eff}) has been proposed that can simulate the observed alloying kinetics. The T_{eff} for the systems studied is found to lie between $0{\cdot}42$–$0{\cdot}52T_l$.**

Keywords. **Nanocrystalline materials; mechanical alloying; alloying mechanism; alloying kinetics.**

1. Introduction

The pioneering work of Benjamin (1970) has led to the evolution of mechanical alloying (MA) as a viable solid state processing route. A number of equilibrium phases such as solid solutions, intermetallic compounds and non-equilibrium phases such as amorphous and quasi-crystalline phases (Koch 1991; Murty and Ranganathan 1998) have been synthesized so far by this technique. However, the number of reports on the mechanism of alloying during MA are relatively few in number (Gilman and Benjamin 1983; Atzmon 1988; Martin and Gaffet 1990; Zbiral *et al* 1992; Yavari 1994; Pabi and Murty 1996). The reports on the alloying kinetics during MA are still fewer (Schultz *et al* 1989; Dupeux *et al* 1993; Bhattacharya and Arzt 1993; Pabi *et al* 1998).

In order to draw a comprehensive hypothesis, an extensive study of the formation of solid solutions and intermetallics in Cu–Ni, Cu–Zn, Cu–Al, Nb–Al and Ni–Al systems by MA has been undertaken. The systems are chosen such that the enthalpy of formation (ΔH_f) ranges from slightly positive in Cu–Ni to highly negative in Ni–Al (Hultgren *et al* 1973). The contribution of ternary alloying addition of Fe and Cr on the mode of formation of NiAl phase during MA has also been highlighted.

During MA in ductile and miscible (completely or partially) systems, deformation leads to a change in the thickness of the constituent phases that in turn distorts the concentration profiles. Moreover, the interface also shifts due to concurrent intermixing of the constituent atoms diffusing at different rates. As a result, the MA kinetics transform into a special moving boundary problem. Pabi *et al* (1998) have recently presented, a rigorous numerical solution to this problem based on a iso-concentration contour migration (MICCM) method. In the present report, we will utilize this model to compare the numerical predictions with the experimental data from the Cu–Ni, Cu–Zn and Cu–Al systems to yield a measure of the effective mass transfer rate operating during MA.

2. Experimental

The MA was performed in a high energy planetary ball mill (Fritsch Pulverisette P-5) at a speed of 300 rpm and ball to powder weight ratio of 10 : 1. The elemental blends studied include $Cu_{100-x}Ni_x$ ($x = 50$, 80 at%), $Cu_{100-x}Zn_x$ ($x = 15$, 30, 40, 50, 65, 85 at%), $Cu_{80}Al_{20}$, $Ni_{100-x}Al_x$ ($x = 21$, 25, 50, 65, 75 at%), $Ni_{40}Al_{40}Fe_{20}$, $Ni_{40}Al_{40}Cr_{20}$ and $Nb_{25}Al_{75}$. Milling was carried out in toluene with elemental powders of ≤ 45 μm size at least up to 20 h with tungsten carbide (WC), hardened chrome

*Author for correspondence

steel (CS) and stainless steel (SS) vials. The various stages of alloying during MA were monitored by X-ray diffraction (XRD) analysis of the milled products using Cu-K_α radiation in a Philips PW1710 diffractometer. The average crystallite sizes were estimated from the XRD peak profile analysis by variance method after eliminating the contributions of instrumental broadening and lattice strain (Williamson and Hall 1953).

3. Results and discussion

3.1 *Alloying mechanism*

Figure 1 presents a series of XRD patterns obtained at different stages of milling of $Cu_{50}Ni_{50}$ blend using SS milling media. It is apparent that the Cu and Ni-peaks continuously shift towards each other due to mutual dissolution by MA. Finally, a single phase microstructure evolves as Cu–Ni solid solution following 20 h of milling. Here, progressive broadening of the peaks may be attributed to gradual refinement of the grain sizes. This type of mixing would be referred hereafter as continuous diffusive mixing.

The fact that nanocrystallization is a prerequisite for alloying is clear from figure 2 which shows the XRD patterns of $Cu_{50}Ni_{50}$ milled in WC, CS and SS milling media under identical conditions. While alloying is clearly evident with CS and SS milling media, no alloying could be observed with WC milling media. A closer look at the XRD patterns makes it clear that the peaks are very sharp in the case of WC when compared to the other two. Crystallite size calculations based on the XRD peak broadening using variance analysis have shown that Cu and Ni crystallites are about 20 nm in diameter in case of CS and SS, while they were about 200 nm in case of WC grinding media.

It was clear from the earlier studies (Murty *et al* 1996) that milling in CS and SS media result in Fe contamination. Fe contamination into Cu and Ni can change their work hardening characteristics resulting in more fragmentation than cold welding during milling. This could be the cause for the Cu and Ni crystallites to be much finer in case of CS and SS milling media than those in case of WC media. These results clearly bring out the fact that alloying during MA is promoted only after the constituent elements become nanocrystalline, thus generating short circuit paths (static or mobile) for enhanced diffusion at temperatures much below their melting points.

Figure 3 shows the XRD patterns of $Cu_{85}Zn_{15}$ and $Cu_{15}Zn_{85}$ elemental blends after MA for 0·5 h (Pabi *et al* 1996; Pabi and Murty 1996). It is clearly evident from the figure that irrespective of the composition of the blend, Zn-rich phase, ε, forms first in the early stages of milling. This suggests that alloying in this system is initiated by the diffusion of Cu in Zn. This contradicts the hypothesis of Zbiral *et al* (1992) who proposed that in case an A–B system, where the equilibrium solubility of B in A is negligible and that of A in B is appreciable, alloying during MA occurs by the diffusion of A into B. According to this hypothesis, alloying in Cu–Zn system should occur by the diffusion of Zn in Cu. However, the results of the present work show that diffusion of Zn in Cu occurs only after Cu reaches nanocrystalline state (~ 15 nm) (figures 4a and b), while the diffusion of Cu in Zn and the formation of Zn-rich phase occurs even when Zn is much coarser in its crystallite size (> 100 nm). Figures 4a and b clearly show

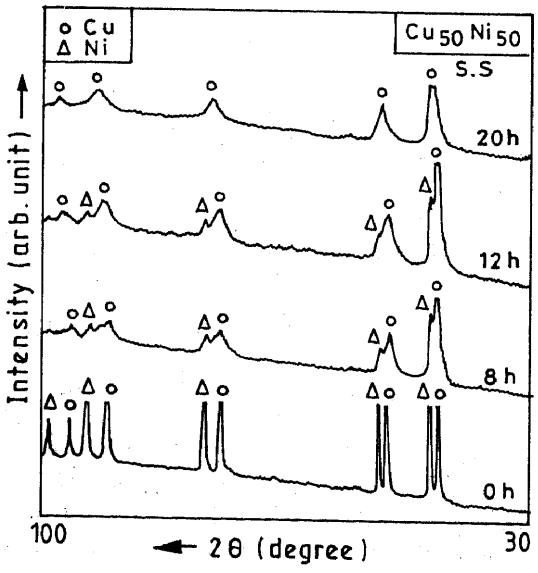

Figure 1. XRD patterns of $Cu_{50}Ni_{50}$ at different stages of milling in SS vial.

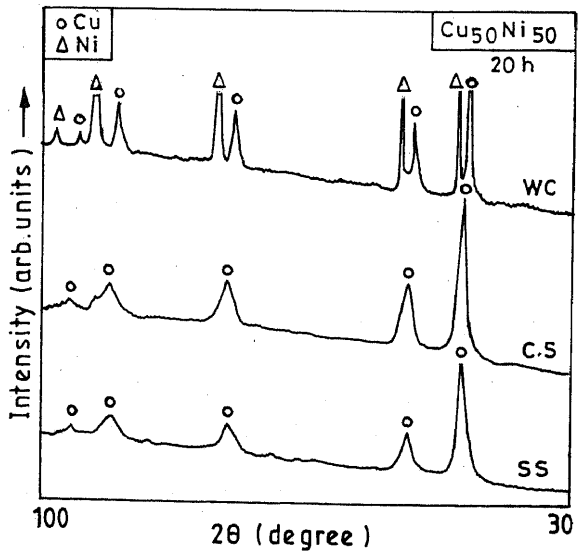

Figure 2. XRD patterns of $Cu_{50}Ni_{50}$ after 20 h of MA in WC, CS and SS milling media.

that, irrespective of the nominal composition of the blend, no significant diffusion of Zn into Cu and a resultant XRD peak shift of Cu were observed until Cu reached about 15–20 nm. Once crystalline size reached this critical limit, rapid shift of the XRD peak of Cu was observed evidencing pronounced diffusion of Zn in Cu.

These results can be understood based on the diffusivities of Cu and Zn in each other. It is clear from the earlier studies (Schwarz and Koch 1986; Davies *et al* 1988) that the temperature rise during ball milling is not appreciable. Assuming that the temperature during milling to be about 200°C, the diffusivities of Cu in Zn and Zn in Cu have been extrapolated from high temperature data (Weast 1995) as $3{\cdot}0 \times 10^{-18}$ and $8{\cdot}2 \times 10^{-27}$ m^2/s, respectively. Since the diffusivity of Cu in Zn is about eight orders higher than that of Zn in Cu, alloying is expected to be initiated by the diffusion of Cu in Zn and the formation of Zn-rich phases such as ε and γ. Diffusion of Zn in Cu and the formation of Cu-rich α phase occurs only after Cu becomes nanocrystalline so that short circuit paths are generated for enhanced diffusion. It can be concluded that alloying in Cu–Zn system also follows continuous diffusive mixing mechanism.

Alloying in Cu–Al system ($Cu_{80}Al_{20}$) also followed continuous diffusive mixing as evidenced by the continuous shift of XRD peaks of Cu while the Al peak positions practically remained unchanged. This suggests that alloying in this system is controlled by the diffusion of Al into Cu.

In Ni–Al system, the metastable equilibrium after MA was the same in all the compositions containing up to 70 at% Al irrespective of the starting ingredients being either blends of pure metals or a prealloyed powder blended with Ni or Al. The extent of crystallite refinement in the Ni–Al intermetallics has been quite significant when compared to Cu–Zn intermetallics, possibly due to the relatively brittle nature and higher melting points of the Ni–Al intermetallics as compared to the various intermetallic phases of Cu–Zn system. The finest of the Ni–Al intermetallics was the NiAl phase (~ 5 nm) at the NiAl–Ni_3Al metastable phase boundary ($Ni_{65}Al_{35}$), while the smallest crystallite size in Cu–Zn system was observed for α phase in $Cu_{50}Zn_{50}$, which is close to the metastable α–β phase boundary composition. This suggests restricted growth of the crystallites due to the mutual hindrance in the two-phase product.

Studies on Ni–Al system revealed contrasting alloying behaviour in Ni_3Al as against NiAl and $NiAl_3$. In the as-milled state, the Ni_3Al was disordered. During its formation, the lattice parameter of Ni gradually changed (as indicated by the continuous XRD peak shifts of Ni) to that of Ni_3Al, suggesting continuous diffusive mixing mechanism to be operative in this case. It is also interesting to note that no significant XRD peak shift could be observed for Al in this case, suggesting that formation of disordered Ni_3Al is controlled by the diffusion of Al in Ni and not *vice versa*. This is in agreement with the hypothesis of Zbiral *et al* (1992) as in this system the equilibrium solid solubility of Ni in Al is much smaller than that of Al in Ni. However, it should be noted that the alloying behaviour with respect to the diffusing species during the formation of disordered Ni_3Al and that in Cu–Zn system is contradictory to each other.

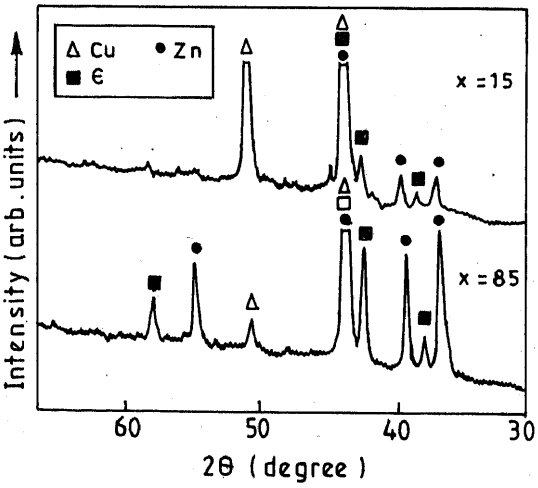

Figure 3. XRD patterns of $Cu_{85}Zn_{15}$ and $Cu_{15}Zn_{85}$ after 0·5 h of MA.

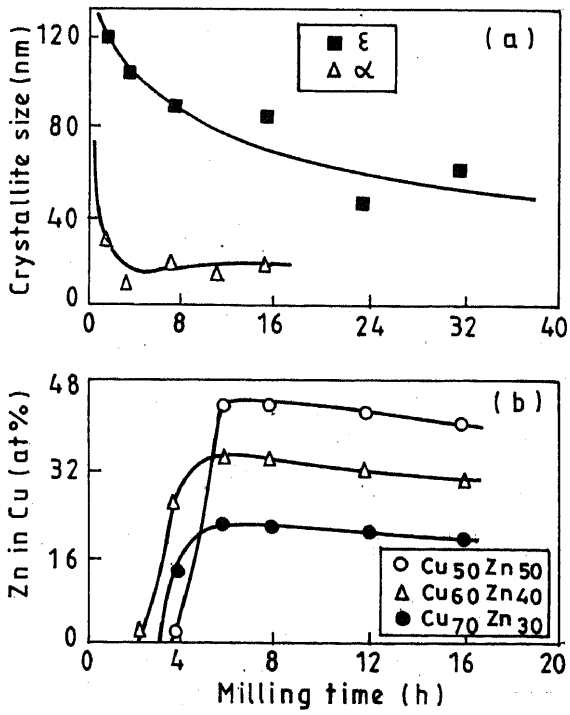

Figure 4. Change in (**a**) crystallite size of Cu and Zn and (**b**) amount of Zn in Cu with milling time.

On the other hand, during the formation of ordered $NiAl_3$ and NiAl, insignificant shift in Ni or Al XRD peaks occurred prior to the formation of these phases. The phases were observed to form all of a sudden when the crystallite sizes of the constituent elements reached a critical nanocrystalline state (figures 5a and b). Interestingly, the crystallite size of the intermetallic at the onset of its formation was equal to the sum of the individual crystallite sizes of the two elements at that stage (figures 5a and b). This is a new mechanism of mixing which has not been observed earlier and is referred to as discontinuous additive mixing (Pabi and Murty 1996) as there exists a discontinuity in the crystallite sizes of the reactants and the product and also as the crystallite size of the product can be obtained by the addition of that of the reactants.

This mechanism is, in a way, similar to the self propagating high temperature synthesis reaction wherein elemental blends are ignited to initiate a reaction between them, leading to the formation of intermetallic compounds. It appears that during the formation of these ordered intermetallics by MA the nanocrystalline nature of the constituent elements provides the required activation energy for the initiation of the reaction and the enthalpy released during the formation of the compound sustains the reaction to its completion. This is further supported by the observation that the critical crystallite size of the constituent elements during the formation of NiAl is higher at the equiatomic composition and decreases on either side. This can be attributed to the decrease in the enthalpy of formation of NiAl on deviation from equiatomic composition. The higher the enthalpy of formation of the compound, the lower is the activation energy for its formation and hence the reaction can initiate even if the constituent elements are slightly coarser than in cases where the enthalpy of formation is lower.

When the as-milled NiAl was made disordered by the ternary additions of Fe or Cr, the alloying mechanism changed from discontinuous additive mixing mode to continuous diffusive mode as exemplified by the variation in the crystallite sizes with milling time for $Ni_{40}Al_{40}Cr_{20}$ (figure 6). It is of interest to note, that the disordered NiAl produced by MA of ternary blends, namely, $Ni_{40}Al_{40}(Fe/Cr)_{20}$, was coarser when compared to the partially ordered binary NiAl synthesized under identical conditions. Such difference in the extent of refinement can be attributed to the change in the deformation behaviour in NiAl due to the introduction of disorder, which is expected to trigger additional slip systems (Noebe *et al* 1993).

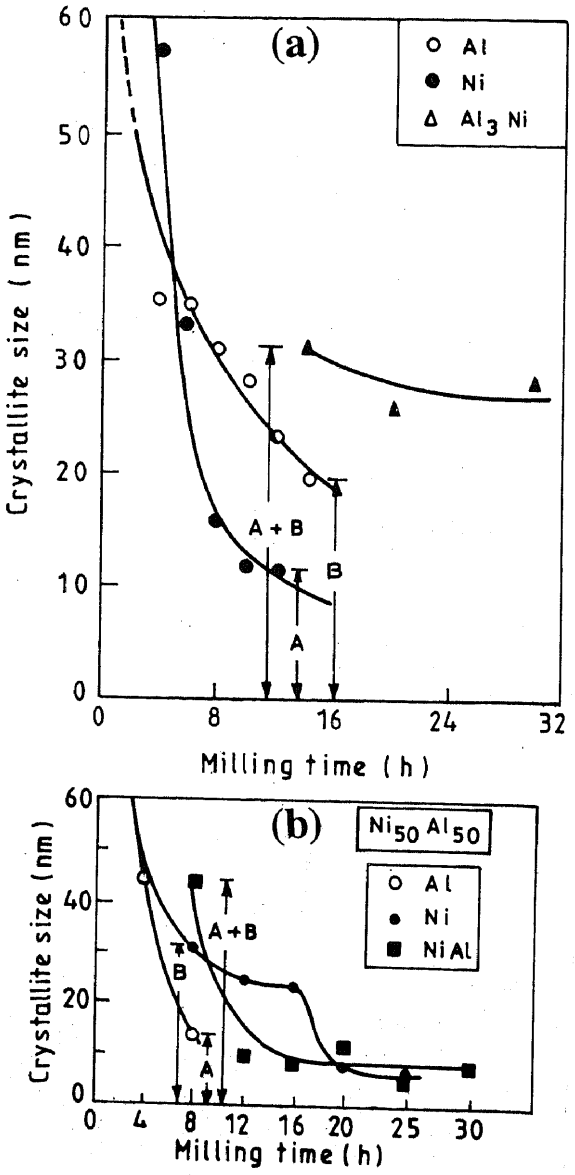

Figure 5. Variation of crystallite size during the formation of (**a**) $NiAl_3$ in $Ni_{21}Al_{79}$ blend and (**b**) NiAl in $Ni_{50}Al_{50}$ blend.

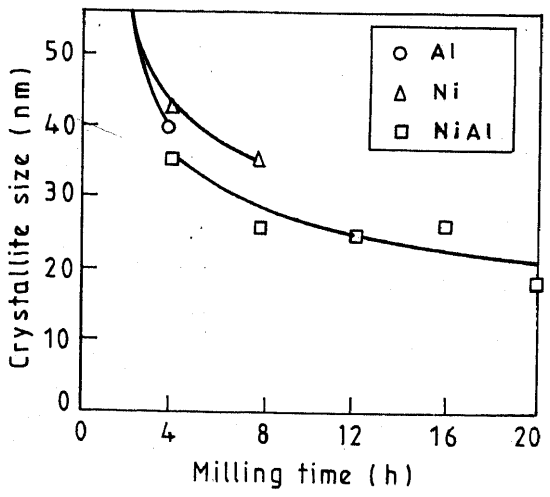

Figure 6. Variation of crystallite size during MA in $Ni_{40}Al_{40}Cr_{20}$ during the formation of NiAl.

In Nb–Al system, the formation of ordered $NbAl_3$ has been observed during MA of an elemental blend of $Nb_{25}Al_{75}$ by continuous diffusive mechanism (figure 7). In this case, with increase in milling time, a continuous shift in the XRD peaks of Nb was observed while the position of Al peaks remained almost unchanged. Thus, the alloying in this case occurs by the diffusion of Al in Nb. This is similar to the observation made in the case of Ni_3Al wherein the alloying was controlled by the diffusion of Al in Ni. However, it is interesting to note that, though $NbAl_3$ formed during MA was ordered it still followed continuous diffusive mixing, instead of discontinuous additive mixing.

A closer look at the results of all the systems reported here suggests that continuous diffusive mixing occurs when the enthalpy of formation and the ordering energy of the phase is small (table 1). Cu–Ni is an isomorphous system with slight positive enthalpy of mixing of about 2 kJ/mol. In addition, the diffusivities of Cu and Ni in each other are not large at the operating temperature during milling and hence nanocrystallization becomes a prerequisite for alloying in this system. In the case of Cu–Zn system, though the enthalpy of formation of the electron compounds is negative, it is quite small (– 8 kJ/mol) and alloying occurs by continuous diffusive mixing. However, due to large differences in the diffusivities of Cu and Zn in each other, alloying is initiated by the faster diffusing element. In case of Ni_3Al, though the enthalpy of formation is quite large (– 42 kJ/mol), the ordering energy is quite small (– 5 kJ/mol) and hence its formation follows the same mechanism as that of a solid solution. In the case of $NbAl_3$, though it is ordered in the as milled state, its relatively low enthalpy of formation (–20 kJ/mol) does not favour discontinuous additive mixing over the conventional continuous diffusive mixing in the nanocrystalline state. It is interesting to note that in all the three systems studied which contained Al (Cu–Al, Ni–Al and Nb–Al), alloying is controlled by the diffusion of Al, when the alloying occurs by continuous diffusive mode.

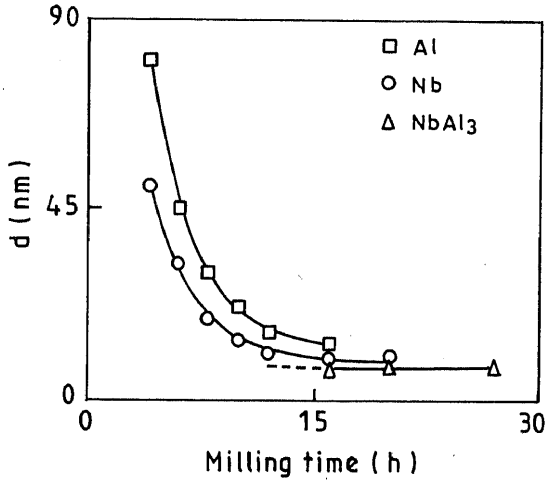

Figure 7. Variation of crystallite size with milling time in $Nb_{25}Al_{75}$ during the formation of $NbAl_3$.

In case of ordered NiAl and $NiAl_3$, which are known to have highly negative values of enthalpy of mixing (table 1), phase formation follows discontinuous additive mixing. The present results of MA suggest that discontinuous additive mode of mixing is favoured only when the enthalpy of formation is highly negative (≤ -40 kJ/mol), as well as, the product phase is ordered. In other words, here, both the above mentioned conditions seem to be the necessary criteria for discontinuous additive mixing.

3.2 *Alloying kinetics*

It is known well over three decades that mechanical deformation enhances the diffusion rate and the process has been termed as 'mechanical interdiffusion' by Balluffi

Table 1. Alloying mechanism in the different systems during MA.

System	Composition	Product phases	C.S. (nm)	Product nature	ΔH_f (kJ/mol)	Alloying mechanism
Cu–Ni	$Cu_{50}Ni_{50}$	Cu(Ni)	20	DO	2	CD
Cu–Zn	Cu–15 to 50 at%Zn	α	20	DO	–8	CD
	Cu–65 to 85 at%Zn	ε	85	DO	–9	CD
Cu–Al	$Cu_{80}Al_{20}$	Cu(Al)	10	DO	–8	CD
Ni–Al	Ni–21 to 25 at%Al	$NiAl_3$	20	ORD	–39	DA
	$Ni_{50}Al_{50}$	NiAl	10	ORD	–72	DA
	$Ni_{75}Al_{25}$	Ni_3Al	30	DO	–42	CD
Ni–Al–Fe/Cr	$Ni_{40}Al_{40}Fe_{20}$	NiAl	25	DO	–	CD
	$Ni_{40}Al_{40}Cr_{20}$	NiAl	20	DO	–	CD
Nb–Al	$Nb_{25}Al_{75}$	$NbAl_3$	9	ORD	–20	CD

C.S., Crystallite size after 20 h MA; ORD, ordered; DO, disordered; CD, continuous diffusive mixing; DA, discontinuous additive mixing

and Rouff (1962). Gleiter (1967) had shown that a large potential gradient leads to a high rate of diffusion in the vicinity of a dislocation even at temperatures where self-diffusion is not possible. He had also shown that the passage of dislocations through Ni_3Al particles in Ni-rich matrix causes pronounced reversal of solute to the matrix from the precipitates, thus resulting in their dissolution at large deformation. Thus, the deformation enhanced diffusivities can play an important role in deciding the alloying kinetics during MA.

In the present work, the MA kinetics have been modeled based on a modified version of the iso-concentration contour migration (ICCM) method (Pabi 1979) developed earlier to estimate the rate of diffusion controlled dissolution in a two-phase planar and multi-layered aggregate. This modified ICCM (MICCM) is capable of considering the deformation induced changes in the diffusion distances while calculating the alloying kinetics. Here, the extent or the rate of deformation of the constituent phases need not be identical. For this purpose, the diffusion equations have been suitably transformed to express the distance as a function of concentration and time such that the concentration becomes an independent variable. As the solute concentration at the interface remains constant in a diffusion controlled alloying process, this transformation converts the moving boundary problem into a static boundary one, even in the presence of mechanical deformation accompanying the MA process. In this model, the distance is computed at any time in two discrete steps, at first to consider diffusive intermixing, and subsequently, to incorporate the effect of concurrent deformation accompanying MA.

Figures 8a–c show the experimental and calculated results of the respective variation of solubility of Ni, Al and Zn in Cu for $Cu_{50}Ni_{50}$, $Cu_{80}Al_{20}$ and $Cu_{70}Zn_{30}$, as a function of milling time. These experimental results are obtained from the XRD peak shifts of Cu in the above mentioned elemental blends during MA. The results of the calculations clearly suggest that the effective mass transport operative during MA attains a rate intermediate between that for volume and grain boundary diffusion.

The enhanced diffusion rate in course of the MA process can be considered to be equivalent to that of volume diffusion at some elevated temperature, T_{eff}. The T_{eff} can be determined by matching the experimental values of solid solution rate with the predictions of MICCM model. The results of the present analysis demonstrate that the equation for ballistic diffusion proposed by Martin and Gaffet (1990) is not able to account for the orders of magnitude enhancement in diffusivity encountered in the MA process.

It is also clear from the results of $Cu_{70}Zn_{30}$ that, though the alloying kinetics are remarkably slower at 200 rpm when compared to that at 300 rpm, the T_{eff} changes only marginally from 505 to 520 K when the milling speed changed from 200 to 300 rpm. The large divergence between the T_{eff} values of two Cu-based systems (Cu–Ni and Cu–Zn) under identical milling

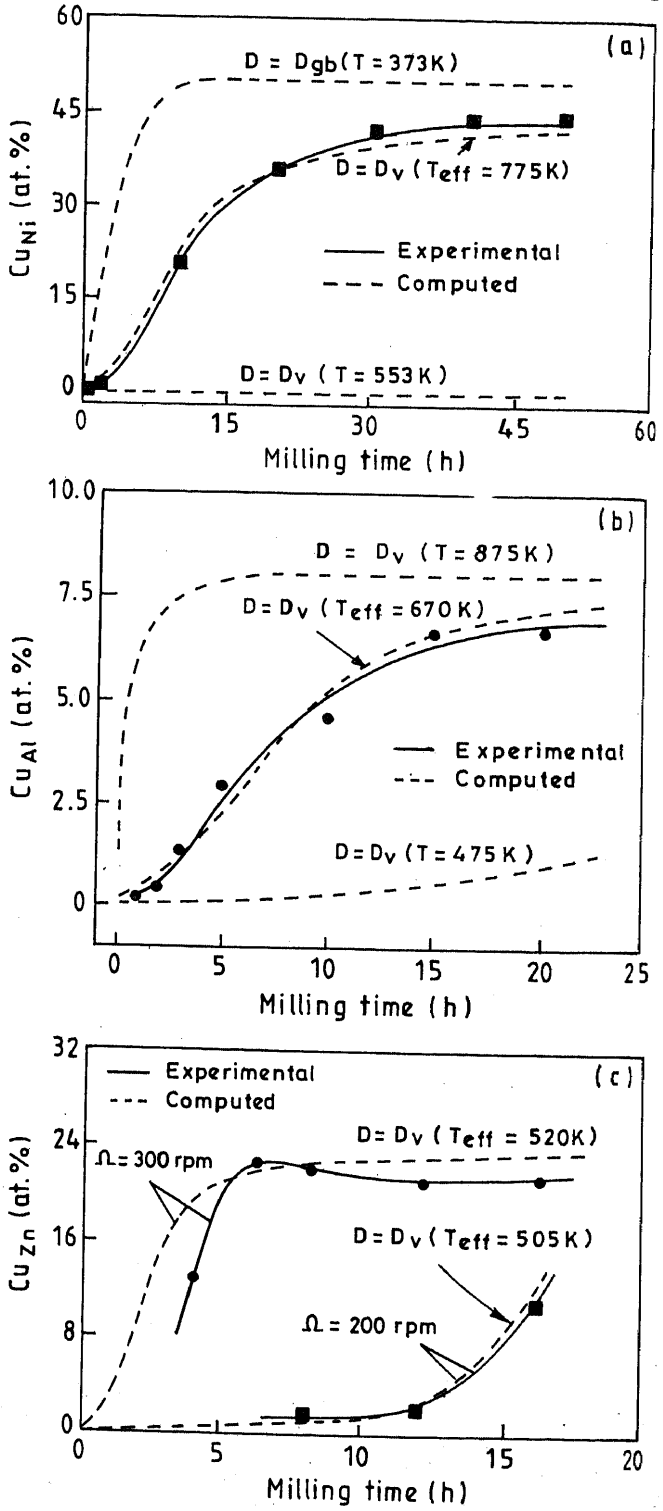

Figure 8. Variation of (**a**) Ni in Cu in $Cu_{50}Ni_{50}$, (**b**) Al in Cu in $Cu_{80}Al_{20}$ and (**c**) Zn in Cu in $Cu_{70}Zn_{30}$ during MA. The solid line represents experimental data and the dotted lines represent calculated values using MICCM model at different T_{eff}.

Table 2. Summary of analysis of the experimental data through MICCM model.

Composition	rpm	T_l(K)	T_{eff}(K)	θ_{eff} (T_{eff}/T_l)
$Cu_{70}Zn_{30}$	200	1217	505	0·42
$Cu_{70}Zn_{30}$	300	1217	520	0·43
$Cu_{60}Zn_{40}$	300	1170	560	0·48
$Cu_{50}Ni_{50}$	300	1580	755	0·48
$Cu_{20}Ni_{80}$	300	1670	785	0·47
$Cu_{80}Al_{20}$	300	1280	670	0·52

conditions indicates that the T_{eff} does not have any direct correlation with the localized temperature rise at the point of ball-powder impact. It is interesting to note that the normalized value of T_{eff} (i.e. θ_{eff}), which is the ratio of T_{eff} and the liquidus temperature of the concerned alloy under consideration (T_l), for all the three systems studied lies in the range of 0·42–0·52 (table 2). Thus, the effective mass transfer rate in MA seems to be related to the liquidus temperature of the system studied. The results may be useful for predicting the alloying kinetics in diverse systems.

4. Conclusions

(I) The mechanism of alloying can be generalized on the basis of enthalpy of formation and ordering energy of the phases.

(II) Continuous diffusive mixing mechanism is operative in case of solid solutions and compounds with low enthalpy of formation, and in case of compounds with high enthalpy of formation, if the as milled product is disordered. Nanocrystallization is a prerequisite for mixing in case of systems with low diffusivities.

(III) The continuous diffusion mixing in Cu–Al and Ni–Al occurs mainly by diffusive in the constituent with higher solubility limit, where it is not so in case of Cu–Zn system.

(IV) Discontinuous additive mixing mechanism operates in the formation of ordered compounds with high enthalpy of formation. However, when these intermetallics become disordered in the as-milled state due to ternary addition, the mechanism of mixing changes from discontinuous additive to continuous diffusive one.

(V) The kinetics of MA analyzed by a iso-concentration contour migration method shows that the effective mass transport rate operative in MA attains a rate equivalent to the volume diffusivity at an elevated temperature T_{eff}.

(VI) T_{eff} is a function of alloy composition and varies marginally with the change in milling speed. T_{eff} does not seem to have any direct correlation with the localized temperature rise at the point of ball to powder impact.

(VII) The ratio of T_{eff} to the liquidus temperature of each alloy studied is found to lie in a very narrow range of 0·42 to 0·52.

Acknowledgements

This work was sponsored by the Department of Science and Technology, New Delhi and the Aeronautical Research and Development Board.

References

Atzmon M 1988 *Phys. Rev. Lett.* **64** 487
Balluffi R W and Rouff A L 1962 *Appl. Phys. Lett.* **1** 59
Benjamin J S 1970 *Metall. Trans.* **1** 2943
Bhattacharya A K and Arzt E 1993 *Scr. Metall.* **28** 395
Davis R M, McDermott B T and Koch C C 1988 *Metall. Trans.* **A19** 2867
Dupeux M, Wan C and Willemin P 1993 *Acta Metall.* **41** 3071
Gilman P S and Benjamin J S 1983 *Ann. Rev. Mater. Sci.* **13** 279
Gleiter H 1967 *Acta Metall.* **16** 455
Hultgren R, Desai P D, Hawkins D J, Gliser M and Kelley K K 1973 *Selected values of thermodynamic properties of binary alloys* (Metals Park, Ohio: ASM) p. 764
Koch C C 1991 *Materials science and technology* (eds) R W Cahn, P Hassen and E Krammer (Weinheim: VCH Publishers) **20** p. 193
Martin G and Gaffet E 1990 *J. Phys. Colloq.* **51** C4–71
Murty B S and Ranganathan S 1998 *Int. Mater. Rev.* **43** 101
Murty B S, Joardar J and Pabi S K 1996 *Nanostructured Mater.* **7** 691
Noebe R D, Bowman R R and Nathal M V 1993 *Int. Mater. Rev.* **38** 193
Pabi S K 1979 *Phys. Status Solidi* **a51** 281
Pabi S K and Murty B S 1996 *Mater. Sci. Eng.* **A214** 146
Pabi S K, Joardar J and Murty B S 1996 *J. Mater. Sci.* **31** 3207
Pabi S K, Das D, Mahapatra T K and Manna I 1998 *Acta Mater.* **46** 3501
Schwarz R B and Koch C C 1986 *Appl. Phys. Lett.* **49** 146
Schultz R, Trudeau M and Huot J Y 1989 *Phys. Rev. Lett.* **32** 2849
Weast R C (ed.) 1995 *CRC handbook of chemistry and physics* (Ohio: CRC Press) 72nd edn. p. F62
Williamson G K and Hall W H 1953 *Acta Metall.* **1** 22
Yavari A R 1994 *Mater. Sci. Eng.* **A179/180** 20
Zbiral J, Jangg G and Korb G 1992 *Mater. Sci. Forum* **88–90** 19